

Distribution of deep-water scleractinian and stylasterid corals across abiotic environmental gradients on three seamounts in the Anegada Passage (#27834)

1

First revision

Guidance from your Editor

Please submit by **15 May 2020** for the benefit of the authors .



Structure and Criteria

Please read the 'Structure and Criteria' page for general guidance.



Raw data check

Review the raw data. Download from the [materials page](#).



Image check

Check that figures and images have not been inappropriately manipulated.

Privacy reminder: If uploading an annotated PDF, remove identifiable information to remain anonymous.

Files

Download and review all files from the [materials page](#).

1 Tracked changes manuscript(s)
1 Rebuttal letter(s)
10 Figure file(s)
7 Table file(s)
1 Raw data file(s)



Structure and Criteria

Structure your review

The review form is divided into 5 sections. Please consider these when composing your review:

1. BASIC REPORTING
2. EXPERIMENTAL DESIGN
3. VALIDITY OF THE FINDINGS
4. General comments
5. Confidential notes to the editor

You can also annotate this PDF and upload it as part of your review

When ready [submit online](#).

Editorial Criteria

Use these criteria points to structure your review. The full detailed editorial criteria is on your [guidance page](#).

BASIC REPORTING

- Clear, unambiguous, professional English language used throughout.
- Intro & background to show context. Literature well referenced & relevant.
- Structure conforms to [Peerj standards](#), discipline norm, or improved for clarity.
- Figures are relevant, high quality, well labelled & described.
- Raw data supplied (see [Peerj policy](#)).

EXPERIMENTAL DESIGN

- Original primary research within [Scope of the journal](#).
- Research question well defined, relevant & meaningful. It is stated how the research fills an identified knowledge gap.
- Rigorous investigation performed to a high technical & ethical standard.
- Methods described with sufficient detail & information to replicate.

VALIDITY OF THE FINDINGS

- Impact and novelty not assessed. Negative/inconclusive results accepted. *Meaningful* replication encouraged where rationale & benefit to literature is clearly stated.
- All underlying data have been provided; they are robust, statistically sound, & controlled.
- Speculation is welcome, but should be identified as such.
- Conclusions are well stated, linked to original research question & limited to supporting results.



The best reviewers use these techniques

Tip

Example

Support criticisms with evidence from the text or from other sources

Smith et al (J of Methodology, 2005, V3, pp 123) have shown that the analysis you use in Lines 241-250 is not the most appropriate for this situation. Please explain why you used this method.

Give specific suggestions on how to improve the manuscript

Your introduction needs more detail. I suggest that you improve the description at lines 57- 86 to provide more justification for your study (specifically, you should expand upon the knowledge gap being filled).

Comment on language and grammar issues

The English language should be improved to ensure that an international audience can clearly understand your text. Some examples where the language could be improved include lines 23, 77, 121, 128 - the current phrasing makes comprehension difficult.

Organize by importance of the issues, and number your points

1. Your most important issue
2. The next most important item
3. ...
4. The least important points

Please provide constructive criticism, and avoid personal opinions

I thank you for providing the raw data, however your supplemental files need more descriptive metadata identifiers to be useful to future readers. Although your results are compelling, the data analysis should be improved in the following ways: AA, BB, CC

Comment on strengths (as well as weaknesses) of the manuscript

I commend the authors for their extensive data set, compiled over many years of detailed fieldwork. In addition, the manuscript is clearly written in professional, unambiguous language. If there is a weakness, it is in the statistical analysis (as I have noted above) which should be improved upon before Acceptance.

Distribution of deep-water scleractinian and stylasterid corals across abiotic environmental gradients on three seamounts in the Anegada Passage

Steven R Auscavitch^{Corresp., 1}, Jay J Lunden¹, Alexandria Barkman¹, Andrea M Quattrini², Amanda W J Demopoulos³, Erik E Cordes¹

¹ Department of Biology, Temple University, Philadelphia, PA, USA

² National Museum of Natural History, Smithsonian Institution, Washington, D.C., United States

³ Wetland and Aquatic Research Center, US Geological Survey, Gainesville, Florida, USA

Corresponding Author: Steven R Auscavitch
Email address: steven.auscavitch@temple.edu

In the Caribbean Basin, the distribution and diversity patterns of deep-sea scleractinian corals and stylasterid hydrocorals are poorly known compared to their shallow water relatives. In this study, we examined species distribution and community assembly patterns of scleractinian and stylasterid corals on three high-profile seamounts within the Anegada Passage, a deep-water throughway linking the Caribbean Sea and western North Atlantic. Using remotely operated vehicle surveys conducted on the E/V *Nautilus* by the ROV *Hercules* in 2014, we characterized coral assemblages and seawater environmental variables between 162-2157 m on Dog Seamount, Conrad Seamount, and Noroît Seamount. In all, 13 morphospecies of scleractinian and stylasterid corals were identified from video with stylasterids being numerically more abundant than both colonial and solitary scleractinians. Cosmopolitan framework-forming species including *Madrepora oculata* and *Solenosmilia variabilis* were present but occurred in patchy distributions among the three seamounts. Framework-forming species occurred at or above the depth of the aragonite saturation horizon with stylasterid hydrocorals being the only coral taxon observed below Ω_{arag} values of 1. Coral assemblage variation was found to be strongly associated with depth and aragonite saturation state, while other environmental variables exerted less influence. This study enhances our understanding of the factors that regulate scleractinian and stylasterid coral distribution in an underreported marginal sea and establishes a baseline for monitoring future environmental changes due to ocean acidification and deoxygenation in the tropical western Atlantic.

1 **Distribution of deep-water scleractinian and**
2 **stylasterid corals across abiotic environmental**
3 **gradients on three seamounts in the Anegada**
4 **Passage**

5
6 Steven R. Auscavitch¹, Jay J. Lunden¹, Alexandria Barkman¹, Andrea M. Quattrini², Amanda W.
7 J. Demopoulos³, Erik E. Cordes¹

8
9 ¹ Department of Biology, Temple University, Philadelphia, PA, USA.

10 ² National Museum of Natural History, Smithsonian Institution, Washington, DC, USA.

11 ³ Wetland and Aquatic Research Center, U.S. Geological Survey, Gainesville, FL, USA.

12

13 Corresponding Author:

14 Steven R. Auscavitch¹

15 steven.auscavitch@temple.edu

16 1900 N 12th St. Philadelphia, PA, 19122, USA.

17

18

19 **Abstract**

20

21 In the Caribbean Basin, the distribution and diversity patterns of deep-sea scleractinian
22 corals and stylasterid hydrocorals are poorly known compared to their shallow water relatives. In
23 this study, we examined species distribution and community assembly patterns of scleractinian
24 and stylasterid corals on three high-profile seamounts within the Anegada Passage, a deep-water
25 throughway linking the Caribbean Sea and western North Atlantic. Using remotely operated
26 vehicle surveys conducted on the E/V *Nautilus* by the ROV *Hercules* in 2014, we characterized
27 coral assemblages and seawater environmental variables between 162-2157 m on Dog Seamount,
28 Conrad Seamount, and Noroît Seamount. In all, 13 morphospecies of scleractinian and
29 stylasterid corals were identified from video with stylasterids being numerically more abundant
30 than both colonial and solitary scleractinians. Cosmopolitan framework-forming species
31 including *Madrepora oculata* and *Solenosmilia variabilis* were present but occurred in patchy

32 distributions among the three seamounts. Framework-forming species occurred at or above the
33 depth of the aragonite saturation horizon with stylasterid hydrocorals being the only coral taxon
34 observed below Ω_{arag} values of 1. Coral assemblage variation was found to be strongly associated
35 with depth and aragonite saturation state, while other environmental variables exerted less
36 influence. This study enhances our understanding of the factors that regulate scleractinian and
37 stylasterid coral distribution in an underreported marginal sea and establishes a baseline for
38 monitoring future environmental changes due to ocean acidification and deoxygenation in the
39 tropical western Atlantic.

40

41 **Introduction**

42 Global and regional modelling efforts in parallel with observational studies have
43 contributed to our understanding of the distribution of framework-forming azooxanthellate corals
44 in the deep sea (>200 m depth). However, a significant number of data deficient localities persist,
45 most often hindered by a lack of records from direct seafloor observation and *in situ*
46 environmental data. A number of environmental variables have been observed to control the
47 distribution of deep-water azooxanthellate scleractinian corals and stylasterid hydrocorals,
48 including parameters linked to depth, terrain, hydrography, and seawater chemistry (Guinotte et
49 al., 2006; Cairns, 2007; Davies & Guinotte, 2011). In the tropical western Atlantic, a center for
50 deep-water scleractinian diversity (Cairns, 2007), additional direct observational data are needed
51 to validate modelling efforts.

52 The growth of a scleractinian coral colony and formation of the aragonitic calcium
53 carbonate skeleton are generally dependent upon the ambient seawater aragonite saturation state
54 (Ω_{arag}) being greater than 1, or supersaturated. However, some deep-water scleractinian corals,

55 including the cosmopolitan species *Solenosmilia variabilis* and *Enallopsammia rostrata*, have
56 been reported well below the saturation horizon (the depth at which $\Omega_{\text{arag}} = 1$) on the Tasmanian
57 Seamounts (Thresher et al., 2011). A more recent survey of seamounts in the Northwestern
58 Hawaiian Islands and Emperor Seamounts documented living colonial scleractinian reefs at Ω_{arag}
59 as low as 0.71 (Baco et al., 2017). Previous studies lend support for targeted observational
60 surveys in underexplored regions in order to delineate species distribution patterns with respect
61 to aragonite saturation and other environmental variables. These efforts are particularly salient in
62 light of potential and ongoing anthropogenic impacts to deep-sea coral ecosystems (Ragnarsson
63 et al., 2017), including global climate change and ocean acidification (Gleckler et al., 2016;
64 Pérez et al., 2018), deep-water drilling and resource extraction (Cordes et al., 2016), bottom-
65 contact fishing (Watling & Norse, 1998), and deep-sea crust mining (Miller et al., 2018).

66 The Greater-Lesser Antilles transition zone is one of the most sparsely surveyed yet
67 biogeographically important deep-water entries from the western Atlantic Ocean into the
68 Caribbean Basin. Topographic features, such as seamounts and other submarine banks associated
69 with deformation along tectonic plate boundaries, are important contributors to the
70 environmental complexity of the deep-sea benthos. In the Anegada Passage, Dog Seamount,
71 Conrad Seamount, Noroît Seamount, and Barracuda Bank are some of the most prominent of the
72 large (> 2km in height above the surrounding seafloor) seamounts and banks present, ranging
73 from abyssal to mesophotic depths. Typical environmental characteristics of seamounts,
74 including substrate heterogeneity, enhanced productivity and carbon flux, and variable currents
75 (Rogers, 2018), create the potential for deep-water biodiversity hotspots in the region and
76 elevated species abundance relative to the adjacent continental margins and slopes. Previous
77 studies indicate that at depths > 200 m, azooxanthellate corals generally prefer hard substrata that

78 exhibit topographic complexity (Roberts et al., 2009; Georgian, Shedd & Cordes, 2014). As
79 such, seamounts are one example of topographically complex deep-water features that provide
80 ideal hard substrate for corals (Rogers, 1994). Yet very few seamount benthic communities in the
81 Caribbean region have been characterized with respect to these important abiotic gradients.

82 Throughout the tropical western Atlantic, scleractinian species diversity and distributions
83 are relatively well-known from shallow waters but the extent of their distribution below 150 m is
84 poorly understood. For deep-water azooxanthellate corals, 81 species have been reported at
85 depths greater than 50 m for the Greater and Lesser Antilles (Cairns, 2007). As with
86 scleractinians, stylasterid hydrocorals are reportedly diverse from the Lesser Antilles (Cairns,
87 1986), can occur in high densities in the tropical western Atlantic (Messing, Neumann & Lang,
88 1990), and are composed of rigid, primarily aragonitic coralla (Cairns & Macintyre, 1992).

89 Additionally, three-dimensional structures produced by deep-water stylasterids provide habitat
90 for fishes (Love, Lenarz & Snook, 2010) and invertebrate fauna (Braga-Henriques et al., 2011;
91 Reed et al., 2013). Efforts have also been made to understand the biogeographic context of
92 Caribbean ecoregions using deep-water corals in order to support conservation strategies (Cairns
93 & Chapman, 2001; Miloslavich et al., 2010; Hernández-Ávila, 2014). In the Caribbean Basin,
94 patterns in deep-sea coral beta diversity (e.g., species turnover) between ecoregions have been
95 attributed to topography and oceanography (Hernández-Ávila, 2014). Within the insular
96 Caribbean, the Greater Antilles and Lesser Antilles regions are found to diverge into two
97 ecoregions, one encompassing the Greater Antilles islands and the other the Lesser Antilles
98 islands, at continental slope depths (200-2000 m) (Hernández-Ávila, 2014). At larger
99 biogeographic scales and evolutionary time, deep-water currents or water masses have been
100 hypothesized as distribution pathways for constraining cosmopolitan habitat-forming corals like

101 *Lophelia pertusa* in the western Atlantic (Arantes et al., 2009; Henry, 2011). While widespread
102 seamount surveys from the Caribbean Basin remain rare, the effect of environmental variables
103 like temperature, dissolved oxygen, and water mass has been demonstrated for demersal fishes
104 on seamounts in the Anegada Passage (Quattrini et al., 2017).

105 The present study focuses on describing patterns in the distribution of deep-water
106 scleractinians and stlyasterid corals on three prominent seamounts in the northeastern Caribbean
107 Sea. In addition to the primary abiotic oceanographic variables including temperature, salinity,
108 and dissolved oxygen, we explore the distribution of aragonitic corals in the region with respect
109 to the aragonite saturation state in this region of the western Atlantic Ocean. As a suspected
110 driver of change in deep-water coral community structure, we also examine the relationship
111 between water mass structure and community similarity in the bathyal zone, hypothesizing that
112 different water masses would have distinct coral assemblages. Finally, we aim to identify abiotic
113 oceanographic variables that most strongly influence the presence of hard corals and their
114 contribution to changes in community similarity for this locality.

115

116 **Materials & Methods**

117

118 *ROV Surveys*

119 This study examined sites within the Anegada Passage in the northeastern corner of the
120 Caribbean Sea (Fig. 1). Three seamounts of varying summit depths were surveyed in September
121 2014 using the ROV *Hercules* during E/V *Nautilus* cruise NA052 (Table 1). Three dives were
122 conducted on Dog Seamount (276 to 1035 m depth), two were conducted on Conrad Seamount
123 (162 to 1314 m depth), and two were conducted on Noroît Seamount (949 to 2206 m depth).

124 Efforts were made to cover similar depth ranges on each feature for direct comparison as
125 permitted by the bathymetry.

126 The ROV was deployed to a maximum target depth on each seamount and generally
127 moved to shallower depths up slope. The ROV continuously traversed the seafloor as near to the
128 bottom as practical at a slow, steady speed (~0.1-0.2 knots, ~0.1 m/s); however, transects were
129 occasionally interrupted by stopping the ROV for sampling and detailed camera zooms. The
130 ROV was equipped with a high-definition camera and paired scaling lasers (10 cm apart). During
131 the dives, the forward-facing cameras were set on wide-angle view, but frequent snap-zooms (up
132 to 20 sec) were conducted to aid in species identification. The ROV was also equipped with a
133 Seabird FastCAT 49 conductivity-temperature-depth (CTD) logger and an Aanderaa oxygen
134 optode to measure dissolved oxygen (DO). The ROV was tracked on the seafloor using an ultra-
135 short baseline (USBL) tracking system as well as a Doppler Velocity Log (DVLNAV).

136

137 *Seawater Collection and Carbonate Chemistry Analysis*

138 Seawater samples ($n = 34$) were collected both in the water column and at the benthos
139 using Niskin bottles mounted to the ROV *Hercules* (Supplementary Table 1). On bottom,
140 seawater samples were collected within 1-2 meters of the benthos and usually co-occurred with
141 the observation of scleractinian colonies on the seafloor. For all seawater samples, co-located
142 physical data (pressure, temperature, salinity, and oxygen) were obtained using vehicle mounted
143 conductivity-temperature-depth (Paroscientific Digiquartz, SBE 49Plus) and oxygen (Aanderaa
144 Optode 3830) sensors, respectively. Upon recovery of the ROV, samples were immediately
145 transferred to 500 mL high-density polyethylene (HDPE) containers according to Best Practices
146 for Ocean CO₂ measurements (Dickson, Sabine & Christian, 2007). While HDPE containers are

147 suitable for long-term storage of seawater for total alkalinity analyses (Huang, Wang & Cai,
148 2012), they are not suitable for long-term storage for pH or dissolved inorganic carbon analyses
149 as they are permeable to CO₂. Accordingly, pH was measured within 1 hour of collection
150 onboard the vessel. Immediately following pH measurement, samples were poisoned with 100
151 μL saturated mercuric chloride solution and stored in a cool, dark location. Total alkalinity was
152 measured in the laboratory in triplicate according to methods previously described (Lunden,
153 Georgian & Cordes, 2013; Georgian et al., 2016a), and final Ω_{arag} values were computed using
154 CO2calc (Robbins et al., 2010). Due to the logistical challenge of pairing a discrete water sample
155 with each individual scleractinian coral observation, we generated a predictive model to
156 interpolate Ω_{arag} at the depth of each coral observation based on temperature, dissolved oxygen,
157 and salinity (for methodology see Georgian et al., 2016a).

158

159 *ROV video analysis*

160 Colonial and solitary coral occurrences were documented using high-definition video
161 transects during each of the ROV dives. Video segments where collections occurred, where the
162 vehicle was too high off the bottom, moving backwards, or of generally poor quality, were
163 removed from analysis. For the purpose of this analysis, we defined structure-forming corals as
164 colonial members of the Scleractinia and hydrozoan family Stylasteridae. Consistent
165 morphospecies identifications were used throughout the analyses. Voucher specimens for
166 morphological identification were obtained using the ROV platform. If necessary, further
167 identifications of coral species were made using taxonomic keys and assistance from taxonomic
168 specialists. Colony height was measured, where possible, by referencing scaling lasers.
169 Individuals or colonies above a 5-cm height threshold were typically identifiable based on laser

170 scalers. If occurrences could not be readily identified below the 5-cm threshold, they were
171 omitted from analysis. Each observation was paired with an associated time-stamp for reference
172 to *in situ* environmental data (temperature, depth, dissolved oxygen concentration, and salinity)
173 collected by ROV CTD and oxygen optode sensors.

174

175 *Community Analyses*

176

177 Sampling effort was evaluated for seamounts individually and for all seamounts combined by
178 sample-based species accumulation curves. In order to assess community relationships among
179 hard-coral assemblages, species abundance values (number of colonies or individuals for each
180 species) were binned into 100 m depth segments for each seamount transect resulting in 28 total
181 samples. Community-level analyses were conducted using standardized and 4th root transformed
182 species abundance data in PRIMER v7 with PERMANOVA add-on (Clarke & Gorley, 2006;
183 Anderson, Gorley & Clarke, 2008). Transformed and standardized species abundances were
184 compiled into a Bray-Curtis resemblance matrix for further analyses. In order to test for
185 significant differences among hard coral assemblages on different seamounts, a one-way analysis
186 of similarity (ANOSIM) was conducted between features as well as between local water masses.
187 Non-metric multidimensional scaling ordinations (nMDS) were conducted across all 28 samples.
188 nMDS plots were overlaid with similarity profile (SIMPROF) analysis to show significant
189 groupings of samples at the 95% level or greater (Clarke, Somerfield & Gorley, 2008). Similarity
190 percentage (SIMPER) tests were used to identify taxa that contributed disproportionately to
191 assemblage similarities within and between seamounts and water masses.

192 Multivariate analyses were also used to explore the abiotic variables relevant to the variation
193 observed in the coral assemblages. Environmental data for temperature, salinity, dissolved
194 oxygen, and Ω_{arag} were obtained from the calculated mean in each 100 m depth segment within

195 every transect. The mean was then 4th-root transformed and normalized within each variable. The
196 BEST (BIO-ENV) routine (Clarke, Somerfield & Gorley, 2008) was applied to the dataset to
197 determine which environmental variables would be useful predictor variables. A distance-based
198 linear model (DistLM) with Akaike information criterion (AIC) was applied using the
199 PERMANOVA add-on in PRIMER v7 (Anderson, Gorley & Clarke, 2008). Visualizations of the
200 resemblance matrix with predictor variables were observed using a dbRDA (distance-based
201 redundancy analysis) ordination with DistLM overlay.

202
203

204 **Results**

205

206 *Survey Summaries*

207 A total of 106 hours of bottom time was assessed across 7 dives (Table 1). Video records
208 were annotated between the depth range of 162-2157 m. In all, 264 observations of solitary and
209 framework-forming scleractinian corals and stylasterid hydrocorals were made across all three
210 seamounts (Table 2). Three dives at Dog Seamount yielded 64 records from 284-849 m. From
211 Conrad Seamount, 182 records were made from 166m to 1230 m across 2 dives. The deepest two
212 dives at Noroît Seamount had 18 records reported from 1014-1626 m. Stylasterids made up the
213 majority (53%) of coral observations, however most were observed at depths shallower than 400
214 m (Table 2). The majority of scleractinians observed were colonial, framework-forming species
215 (100 colonies observed) while only 22 observations were made of solitary coral species, as they
216 were often on or below the threshold for identification. For this reason, abundances of solitary
217 scleractinians represent a minimum value. No scleractinians or stylasterids above the 5 cm size
218 threshold were observed deeper than 1626 m on any seamount.

219

220 *Water Mass Structure*

221

222 Downcast CTD profiles from the ROV sensors were plotted and assessed at each seamount
223 using Ocean Data View v5 (Schlitzer, 2019). Profiles for each seamount were combined to create
224 one consensus profile for the Anegada Passage (Fig. 2). Water masses were identified following
225 published records of temperature, salinity, and dissolved oxygen profiles for the northeast
226 Caribbean and Anegada Passage; these include Subtropical Underwater (SUW) 100-200 m,
227 Sargasso Sea Water (SSW) 200-400 m, Tropical Atlantic Central Water (TACW) 400-700 m,
228 Antarctic Intermediate Water (AAIW) 700-1200 m, and North Atlantic Deep Water (NADW)
229 (>1200 m) (Morrison & Nowlin, 1982; Liu & Tanhua, 2019).

230

231 *Carbonate chemistry analysis*

232 Water samples for carbonate chemistry analyses were collected at depth from 50 m to
233 2170 m. Total alkalinity ranged from 2291.4 to 2405.9 $\mu\text{mol}\cdot\text{kg}^{-1}$, and pH ranged from 7.83 to
234 8.11, with minimum pH observed at 795 m depth. Measured Ω_{arag} values from Niskin bottle
235 collections ranged from 4.13 at 50 m depth to 0.99 at 2170 m depth. The aragonite saturation
236 state of the water column was modelled according to the following equation: $\Omega_{\text{arag}} = (T \times$
237 $0.11407018) + (O \times 0.00302922) + (S \times 0.18168448) - 6.5216044$ (stepwise backward
238 regression, $R^2 = 0.9857$, $p < 0.001$) where T = temperature in $^{\circ}\text{C}$, O = oxygen concentration in
239 $\mu\text{mol}\cdot\text{L}^{-1}$, and S = salinity in parts per thousand (ppt). From this, predicted Ω_{arag} values ranged
240 from 4.11 to 1.05, with highest value at 51 m at Dog Seamount and lowest value at 2195 m at
241 Noroît Seamount.

242

243 *Coral species Distribution Patterns*

244 The single most abundant scleractinian coral species was *Solenosmilia variabilis* (44
245 colonies), but it was only observed on Conrad Seamount in a relatively narrow depth range, 409-
246 569 m. Many structure-forming colonies were found to be associated with boulder and low,
247 outcropping, hard rock substrate. This was followed by the more widespread *Madrepora oculata*
248 (22 colonies), which occurred between 784 and 1540 m on all seamounts (Fig. 3). *Madrepora*
249 *oculata*, which displayed two different growth forms from thin and sparsely branching to thick,
250 robust colonies, possessed the widest depth distribution range for any colonial scleractinian
251 coral. The deepest solitary scleractinian coral, *Javania cailleti*, was observed at 1626 m; this
252 occurrence corresponds with one of the lowest measured Ω_{arag} values of 1.01.

253 The upper bathyal depths, shallower than 700 m, contained species with narrower depth
254 distributions than those at lower bathyal depths (>800 m) (Fig. 3). The sub-700 m assemblage
255 was composed of three species of scleractinians (*E. rostrata*, *M. oculata*, and *J. cailleti*) and one
256 stylasterid (*Crypthelia* sp. 1). The shallowest depths, usually coinciding with the seamount
257 summit, were dominated by two species of stylasterids, *Stylaster* sp. 1 and *Stylaster* cf.
258 *duchassaingi*, as well as one azooxanthellate scleractinian, *Madracis myriaster*. On Conrad
259 Seamount, pink and purple coralline algal crusts were observed as deep as 256 m depth and
260 continued to be observed through shallower depths dominated by sponges, stylasterids, and black
261 corals.

262 The majority of stylasterid species were restricted to depths less than 400 m with only
263 *Crypthelia* exhibiting a wider depth distribution (Fig. 3). Only three morphospecies of
264 stylasterids were large enough to be consistently identified during video annotation. Other
265 unidentifiable stylasterids were combined into a fourth group, Stylasteridae spp. and shown for

266 reference. The most abundant species, *Stylaster* sp. 1, was found in a narrow depth range
267 between 166-174 m on the summit of Conrad Seamount.

268

269 *Patterns of Coral Occurrences with Aragonite Saturation State*

270 Measured Ω_{arag} values from water collected adjacent to corals were not significantly
271 different (t-test, $N=9$, $t=-0.23341$, $p=0.818$) compared to what was calculated using the modelled
272 aragonite saturation state data (Supplementary Fig. 1). All paired water samplings adjacent to
273 coral observations occurred at or above the aragonite saturation horizon ($\Omega_{\text{arag}} > 1$) (Table 3).
274 Multiple water samples for a single species were collected for only *M. oculata*. A full table of all
275 34 Niskin water bottle measurements and matched environmental variables is provided
276 (Supplementary Table 1).

277 Using predicted values derived from CTD and sensor data on temperature, oxygen
278 concentration, and salinity, all scleractinian and stylasterid corals were observed at Ω_{arag} values
279 of 0.99 to 3.45 (Fig. 4). For scleractinians, *Javania cailleti* occurred across the largest aragonite
280 saturation state range, between 1.01 and 1.77. Among the Stylasteridae, *Crypthelia* sp. 1
281 occurred across the greatest range of saturation states from as low as 0.99 up to 2.83. Only three
282 species were observed at or around the aragonite saturation horizon based on predicted saturation
283 state values, *Crypthelia* sp. 1 ($\Omega_{\text{arag}}=0.99$), *M. oculata* ($\Omega_{\text{arag}}=1.00$) and *J. cailleti* ($\Omega_{\text{arag}}=1.01$).

284

285 *Community Structure Patterns*

286 Species-accumulation curves were evaluated for seamounts individually and in aggregate for
287 all seamounts. Combined, all seamounts (100-1700 m) revealed a more complete sampling effort
288 than among single seamount coral assemblages (Fig. 5). Individually, species accumulation

289 curves for Dog, Conrad, and Noroît seamounts were not asymptotic, and therefore are likely to
290 accumulate additional coral species with increased sampling effort.

291 Analysis of similarity (two-way nested, depth within seamount, Global $R=0.122$, $p=0.05$)
292 conducted among seamounts revealed significant differences in coral assemblages between Dog
293 and Noroît Seamounts ($R=0.544$, $p=0.006$), but not Conrad and Dog seamounts ($R=-0.001$,
294 $p=0.379$) or Conrad and Noroît seamounts ($R=0.029$, $p=0.292$) (Supplementary Table 2). A one-
295 way ANOSIM (Global $R=0.464$, $p=0.001$) between water masses revealed significant differences
296 in coral assemblages between SSW and TACW ($R=0.46$, $p=0.003$), AAIW ($R=0.53$, $p=0.002$),
297 and NADW ($R=0.60$, $p=0.008$) as well as between TACW and NADW ($R=0.93$, $p=0.001$) and
298 AAIW and NADW ($R=0.361$, $p=0.01$) (Supplementary Table 3).

299 Non-metric multi-dimensional ordination with SIMPROF groupings revealed five statistically
300 significant groupings; two shallow assemblages composed of 100 m depth-binned samples from
301 between 100-600 m and 200-400 m, two mid-depth assemblages (500-700 m and 700-1100 m),
302 and one deep assemblage (1100-1600 m) (Fig. 6). Outliers from these groupings occurred in the
303 600-700 m and 1100-1200 m depth bins on Conrad Seamount and between 1300-1400 m on
304 Noroît Seamount. Within SIMPROF groupings, the shallowest depth grouping showed the
305 greatest amount of dissimilarity among samples (a metric of beta diversity) among the three
306 seamounts while the lowest occurred in the deepest group.

307 Dog Seamount exhibited the lowest beta diversity of coral assemblages among all three
308 seamounts and the highest average similarity at 61% (one-way SIMPER analysis), with the
309 average similarity between 100 m depth bins being most strongly influenced by *Crypthelia* sp.
310 1, which contributed to 96.6% of the relative abundance. Noroît Seamount had the second
311 highest similarity (38.2%), with *M. oculata* accounting for 84.7% of the similarity. Conrad

312 Seamount had the lowest average similarity (15%), with stylasterids *Crypthelia* sp. 1 and
313 *Stylaster* cf. *duchassaingi* being the greatest contributors to average similarity with 48.4% and
314 21.5%, respectively. Between seamounts, Noroît differed from Dog and Conrad, primarily due to
315 the higher abundance of *M. oculata* at Noroît Seamount. Noroît Seamount had nearly triple the
316 average abundance of *M. oculata* compared to Conrad Seamount. Conrad and Dog Seamounts
317 differed primarily due to the contribution of *Crypthelia* sp. 1 and *M. myriaster*, which were
318 present on Conrad at 2 to 3 times higher average abundance than at Dog Seamount.

319 Within water masses, the greatest average similarity of coral assemblages occurred within
320 NADW (54%) followed by TACW (51%) and finally SSW at (32 %). The abundance of
321 scleractinians was responsible for greater similarities within deep water masses (*M. oculata* and
322 *Javania cailleti* in NADW) while stylasterids were more commonly associated with driving
323 patterns of similarity within intermediate and shallower water masses (*Crypthelia* sp. 1 in
324 TACW, AAIW and *Stylaster* cf. *duchassaingi* in SSW). Between immediately adjacent water
325 masses, the greatest average dissimilarity was observed between SUW and SSW (92.3%) and the
326 lowest between TACW and AAIW (56.7%), indicating higher rates of turnover (beta diversity)
327 for shallower water masses than deeper ones.

328 Results from the BEST analysis indicated that the largest percentage of biological variation
329 was correlated with depth ($r=0.536$). The BEST routine also indicated that the greatest
330 correlation occurred with the four combined factors of depth, Ω_{arag} , temperature, and dissolved
331 oxygen ($r=0.614$). Sequential tests in the DistLM analysis indicated that depth (AIC=223.88,
332 $p=0.001$) and Ω_{arag} (AIC= 215.87, $p=0.001$) were the greatest explanatory variables influencing
333 coral assemblages on seamounts in the Anegada Passage. Temperature, salinity, and oxygen did
334 not explain a significant portion of the biological variation in this test. Redundancy analyses

335 resulted in 59.4% of the DistLM model variation explained by the primary axis (dbRDA1) and
336 32.6% explained by the second (dbRDA2) (Fig. 7). Likewise, the first axis explained 32.8% of
337 the total biological variation observed and the second axis explained 18%. The primary axis was
338 most closely correlated with oxygen ($r = -0.82$), while the second was most closely related to
339 temperature ($r = -0.61$).

340

341

342 Discussion

343 Seamounds in the Anegada Passage were found to harbor communities of stony and lace
344 corals throughout the bathyal depth range from summit depths as shallow as 166 m to a
345 maximum of 1626 m. Both stylasterid and scleractinian coral species with aragonitic skeletons
346 were largely present above the aragonite saturation horizon in this region of the western Atlantic
347 Ocean, with the understanding that sampling effort below the ASH was limited to one transect at
348 Noroît Seamount (Table 1). Nevertheless, we were able to identify the depth of the ASH as
349 occurring between 2000-2200 m in the Anegada Passage (Supplementary Fig. 1), which is
350 consistent with previous reports from the North Atlantic Ocean (Jiang et al., 2015). Only
351 stylasterids in the genus *Crypthelia* were observed to occur below the aragonite saturation
352 horizon ($\Omega_{\text{arag}} = 0.99$), but others, including the framework-forming species *Madrepora oculata*,
353 occurred at saturation states as low as $\Omega_{\text{arag}} = 1.0$. However, it is likely that aragonitic corals live
354 below the aragonite saturation horizon within our study region, as our sampling effort was lower
355 at these depths. Also noteworthy was the observation of live crustose coralline algae at a depth of
356 256 m, which is comparable to the deepest known record from San Salvador Island (268 m) in
357 The Bahamas (Littler et al., 1986).

358 Overlying water masses were a significant indicator of community assembly differences
359 between SSW (Sargasso Sea Water) and deeper water masses, but not the shallowest water mass,
360 Subtropical Underwater (SUW) and deeper strata of the water column. Oceanographic variables
361 that most strongly influenced the presence of aragonitic corals and their contribution to changes
362 in community similarity were depth and aragonite saturation state, with temperature, salinity, and
363 dissolved oxygen making less significant contributions.

364 The tropical western Atlantic is a known diversity center for azooxanthellate scleractinian
365 corals and stylasterid hydrocorals (Cairns, 2007, 2011). This study provides new distribution
366 records for deep-water coral species in the northeastern Caribbean and builds on existing efforts
367 to characterize the azooxanthellate coral fauna of the tropical western Atlantic (Cairns, 1979;
368 Cairns & Chapman, 2001; Lutz & Ginsburg, 2007). Specifically, 7 species or morphospecies of
369 stony corals within the genera *Javania*, *Madrepora*, *Madracis*, *Enallopsammia*, *Dendrophyllia*,
370 and *Caryophyllia* have been added to local species inventories in the Anegada Passage (Fig. 8).
371 New records from photographic and physical specimens aid in resolving the complex
372 biogeography of the Greater-Lesser Antilles Transition zone seamounts with respect to the
373 western North Atlantic (Supplementary Table 4). The paucity of records paired with
374 environmental parameters from global biogeographic databases makes these observations critical
375 to understanding the species distribution dynamics of marginal Atlantic seas and how coral
376 distribution may be affected by future ocean climatic changes.

377 Stony coral assemblages in the Anegada Passage were similar to those observed in other
378 parts of the western Atlantic Ocean with a few noteworthy absences. Absent from our records
379 from the Anegada Passage seamounts include reef-forming species like *L. pertusa* and *E.*
380 *profunda*, as well as cosmopolitan cup coral species like *Desmophyllum dianthus*, which are

381 reportedly more common throughout the U.S. southeast continental shelf and Gulf of Mexico
382 (Schroeder et al., 2005; Reed, Weaver & Pomponi, 2006; Brooke & Schroeder, 2007; Lunden,
383 Georgian & Cordes, 2013; Georgian et al., 2016a). While fossilized *Lophelia* rubble have been
384 reported in the Colombian Caribbean (Santodomingo et al., 2007) and live *Lophelia* has been
385 observed on the Brazilian continental margin (Arantes et al., 2009), the southern Caribbean
386 (Hernández-Ávila, 2014), and off Roatan, Honduras (Henry, 2011), members of this genus have
387 not been extensively reported in the insular Caribbean (OBIS, 2019).

388 We were also able to identify some variability in local distribution patterns among
389 seamounts for three colonial scleractinian species. *Enallopsammia rostrata*, *Dendrophyllia*
390 *alternata*, and *Solenosmilia variabilis* appear to have patchy distributions on the Anegada
391 Passage seamounts. For example, only two colonies of *E. rostrata* were observed, both on Dog
392 Seamount at 785m, and only five colonies of *D. alternata* were observed on Conrad Seamount
393 between 490-598 m (Fig. 3). Similarly, *S. variabilis* was only observed in patches on Conrad
394 Seamount from 490-569 m (Fig. 3). *Solenosmilia* has not been widely reported from the greater
395 Caribbean basin based on records from the Ocean Biogeographic Information System (OBIS,
396 2019), but is known to be a contributor to coral mound formation off Brazil (Raddatz et al.,
397 2020). *Solenosmilia* has been more commonly reported to asexually reproduce, and thus has a
398 relatively short dispersal ability (Miller & Gunasekera, 2017), potentially explaining its patchy
399 distribution.

400 Several coral taxa encountered in the Anegada Passage are important species for
401 understanding biogeographic patterns of the Caribbean bathyal zone. *Madracis myriaster* was
402 observed both on Dog and Conrad Seamounts, but only between 253 - 311 m. More recently, *M.*
403 *myriaster* has been observed at similar depths and in high densities during surveys by the ROV

404 *Deep Discoverer* on the NOAA Ship *Okeanos Explorer* east of Vieques Island and in the Mona
405 Passage at similar depths (Wagner et al., 2019). Northern and eastern Caribbean coral
406 communities at continental shelf depths have been found to be dissimilar from the southern
407 Caribbean, such that they may constitute distinct ecoregions (Hernández-Ávila, 2014). These
408 differences were found to be driven by differences in the abundance of *M. myriaster* (Fig. 8C),
409 which is more common at mesophotic and upper bathyal depths (Reyes et al., 2005;
410 Santodomingo et al., 2007; Hernández-Ávila, 2014). At lower bathyal depths, regional
411 biogeographic differences have also been attributed to variation in the frequency of solitary
412 scleractinian species (e.g. *Stephanocyathus* spp., *Fungiacyathus* sp.) that may be difficult to
413 detect during video transects (Hernández-Ávila, 2014). A greater diversity of solitary
414 scleractinian corals and smaller stylasterids may have been present in the video but could not be
415 documented due to limitations of ROV surveys (discussed in Everett & Park, 2018). The lack of
416 easily identifiable diagnostic features from video, rugose terrain (e.g. overhangs and ledges), and
417 rarity make most smaller species difficult to identify from ROV surveys without voucher
418 specimens. A more thorough analysis incorporating modern (e.g. higher-resolution ROV video
419 surveys with *in situ* collections) and historical datasets (e.g. museum-archived specimens) would
420 be helpful in elucidating biogeographic patterns more broadly across the basin.

421 Several species in the genus *Crypthelia* occur in the eastern Caribbean at bathyal depths
422 (Cairns, 1986). The difficulty of identifying stylasterids from ROV video remains a challenge in
423 establishing species occurrences, necessitating a voucher collection to confirm morphospecies
424 identity. Nevertheless, the depth distribution, colony morphology, and coloration of *Stylaster* sp.
425 1, is consistent with *Stylaster roseus* (Pallas, 1766), a tropically-distributed western Atlantic
426 stylasterid from depths typically less than 500 m (OBIS, 2019). *Crypthelia* sp. and other

427 stylasterid species are more likely to be underreported due to their small size (2-5 cm), on the
428 threshold of being able to be accurately recorded from ROV video. These stylasterids were also
429 observed under overhangs which made obtaining an accurate account of their abundance
430 difficult. In this case, the reported occurrences of these corals represent a minimum value.

431 The ecological contribution of stylasterid corals is often understated, despite the ability of
432 some species to produce significant three-dimensional structures that can act as habitat for other
433 organisms. Larger structure-forming stylasterids are functionally analogous to some colonial
434 scleractinian corals in that they can provide habitat for larger organisms such as deep-water
435 fishes and invertebrates (Love, Lenarz & Snook, 2010; Braga-Henriques et al., 2011). *Crypthelia*
436 spp., while relatively abundant in places and occurring over a wide range, were never observed
437 above 12 cm in overall height and were observed to be extremely brittle when attempting
438 collection (Fig. 9A). However, two species in the genus *Stylaster*, *S. cf. duchassaingi* (Fig. 9B)
439 and *Stylaster* sp. 1 (Fig. 9C), can be classified as potentially important three-dimensional
440 structure-forming species, primarily occurring between 150- 400 m depth.

441 The carbonate mineralogy of most stylasterids is similar to scleractinians in that a
442 majority of known species, including those observed in this study, produce a skeleton composed
443 primarily of the mineral aragonite (Cairns, 2011), although some are calcitic in composition
444 (Cairns & Macintyre, 1992). Stylasterids do share distribution characteristics and overlapping
445 depth ranges with many upper bathyal solitary and colonial scleractinian corals (Cairns, 1986,
446 2011). Like scleractinians, stylasterid hydrocorals also exhibit a vulnerability to changing
447 aragonite saturation conditions over their depth distribution (Guinotte et al., 2006).

448

449 Knowledge of the chemical environment of deep-sea scleractinians has grown
450 significantly in recent years as empirical measurements of the carbonate system at deep-sea coral
451 habitats have been reported from different regions across the global ocean. On seamounts in the
452 Indian Ocean off the coast of SW Australia, the majority of framework-forming scleractinians –
453 including *E. rostrata* and *S. variabilis* – were found at Ω_{arag} values at or just below saturation,
454 suggesting a control on the lower limit of these species' distributions (Thresher et al., 2011).
455 However, live scleractinian reefs were recently discovered on seamounts in the North Pacific at
456 Ω_{arag} values as low as 0.71 (Baco et al., 2017) and as low as 0.81 off Southern California (Gómez
457 et al., 2018). Additionally, scleractinians have been observed below the ASH in the Indian Ocean
458 (Trotter et al., 2019) and South Atlantic Ocean (Barbosa, Davies & Sumida, 2020). These
459 revelations indicate that, under the right conditions, scleractinian corals can persist in
460 undersaturated waters (Baco et al., 2017). Additionally, the presence of live tissue may buffer
461 against the effects of low pH (Venn et al., 2011), but the underlying dead coral framework may
462 be less resilient to undersaturated waters. Expanded surveys below 2000 m in northern
463 Caribbean, in tandem with additional effort in sampling of coral-adjacent deep-waters for
464 carbonate chemistry analysis will aid in better determining the controls on aragonitic coral
465 species distribution at lower bathyal depths in the tropical western Atlantic.

466 Productivity of the surface waters and export to the deep-sea benthos may contribute to
467 differences in species distribution and abundance of deep-sea corals. In a 2016 laboratory
468 experiment and field study comparing two spatially distinct and genetically isolated populations
469 of the framework-forming scleractinian *Lophelia pertusa*, colonies from Norway exhibited
470 enhanced respiration and prey capture rates under acidified conditions compared to individuals
471 from the Gulf of Mexico (Georgian et al., 2016b). This study lends support to the hypothesis that

472 species are locally adapted to environmental conditions, including food supply, which may allow
473 individuals to better tolerate reduced carbonate saturation states.

474 **Conclusions**

475
476 Our results offer some insights to the distribution, diversity, and drivers of community
477 assembly of scleractinian and stlyasterid deep-water corals in a data-deficient region of the
478 tropical western Atlantic Ocean. These findings lend support for the efficacy of targeted
479 exploration surveys to understand coral distribution with respect to environmental gradients in
480 the deep-sea environment. The presence of aragonitic corals, largely occurring above the
481 aragonite saturation horizon, was not unexpected, but more surprising was the presence of
482 known framework-forming scleractinians, like *Madrepora oculata*, living at or just above Ω_{arag}
483 =1 in this locality. Future work should seek to expand upon coral community inventories for this
484 area to include members of the Octocorallia and Antipatharia, particularly to refine the
485 relationship between community assembly and water mass structure. Increased taxonomic effort
486 is needed to better identify cryptic coral morphospecies from the deep-sea benthos, and
487 particularly for those size classes below the identification threshold for ROV video surveys. In
488 the Atlantic Ocean, deep-water coral ecosystem health is likely to be negatively impacted by
489 environmental change by the end of the current century. Warming deep-waters (Gleckler et al.,
490 2016), thermohaline driven deep-water acidification (Pérez et al., 2018), and low latitude
491 deoxygenation in the Atlantic (Montes et al., 2016) are among the greatest threats facing deep-
492 water framework-forming corals. The relationship between coral occurrences and environmental
493 variables reported here establish a critical baseline for the detection of the effects of deep ocean
494 change to seafloor communities, which is crucial to effective conservation.

495

496 **Acknowledgements**

497

498 We would like to thank the efforts of the science party, master, and crew of the E/V *Nautilus* on
499 *Exploration of the Anegada Passage* (NA052). We would like to extend a special thanks to the
500 Ocean Exploration Trust for their support. Taxonomic assistance in identifying voucher material
501 was provided by Stephen Cairns (NMNH) for scleractinian and stylasterid corals. We would also
502 like to thank Jason Chaytor, Alex Rogers, Iván Hernández-Ávila, and Nadia Santodomingo for
503 their feedback in the revision of this manuscript. Any use of trade, firm, or product names is for
504 descriptive purposes only and does not imply endorsement by the U.S. Government.

505

506 **References**

507

508 Anderson M, Gorley RN, Clarke RK. 2008. *Permanova+ for Primer: Guide to Software and*
509 *Statistical Methods*. Primer-E Limited.

510 Arantes RCM, Castro CB, Pires DO, Seoane JCS. 2009. Depth and water mass zonation and
511 species associations of cold-water octocoral and stony coral communities in the
512 southwestern Atlantic. *Marine Ecology Progress Series* 397:71–79. DOI:
513 10.3354/meps08230.

514 Baco AR, Morgan N, Roark EB, Silva M, Shamberger KEF, Miller K. 2017. Defying
515 Dissolution: Discovery of Deep-Sea Scleractinian Coral Reefs in the North Pacific.
516 *Scientific Reports* 7:1–11. DOI: 10.1038/s41598-017-05492-w.

517 Barbosa R V, Davies AJ, Sumida PYG. 2020. Habitat suitability and environmental niche
518 comparison of cold-water coral species along the Brazilian continental margin. *Deep Sea*
519 *Research Part I: Oceanographic Research Papers* 155:103147.

520 Braga-Henriques A, Carreiro-Silva M, Porteiro FM, De Matos V, Sampaio Í, Ocaña O, Ávila SP.

- 521 2011. The association between a deep-sea gastropod *Pedicularia sicula* (Caenogastropoda:
522 Pediculariidae) and its coral host *Errina dabneyi* (Hydrozoa: Stylasteridae) in the Azores.
523 *ICES Journal of Marine Science* 68:399–407. DOI: 10.1093/icesjms/fsq066.
- 524 Brooke S, Schroeder WW. 2007. State of deep coral ecosystems in the Gulf of Mexico region:
525 Texas to the Florida Straits. *The State of Deep Coral Ecosystems of the United States*:271–
526 306.
- 527 Cairns SD. 1979. The deep-water Scleractinia of the Caribbean Sea and adjacent waters. *Studies*
528 *on the Fauna of Curaçao and other Caribbean Islands* 57:1–341.
- 529 Cairns SD. 1986. A revision of the northwest Atlantic Stylasteridae (Coelenterata: Hydrozoa).
530 *Smithsonian Contributions to Zoology*:1–131. DOI: 10.5479/si.00810282.418.
- 531 Cairns SD. 2007. Deep-water corals: An overview with special reference to diversity and
532 distribution of deep-water scleractinian corals. In: *Bulletin of Marine Science*.
- 533 Cairns SD. 2011. Global diversity of the stylasteridae (Cnidaria: Hydrozoa: Athecatae). *PLoS*
534 *ONE* 6. DOI: 10.1371/journal.pone.0021670.
- 535 Cairns SD, Chapman RE. 2001. Biogeographic affinities of the North Atlantic deep-water
536 Scleractinia. *Proceedings of the First International Symposium on Deep-Sea Corals*.
- 537 Cairns SD, Macintyre IG. 1992. Phylogenetic implications of calcium carbonate mineralogy in
538 the Stylasteridae (Cnidaria: Hydrozoa). *Palaios*:96–107.
- 539 Clarke KR, Gorley RN. 2006. User manual/tutorial. *PRIMER-E Ltd., Plymouth*.
- 540 Clarke KR, Somerfield PJ, Gorley RN. 2008. Testing of null hypotheses in exploratory
541 community analyses: similarity profiles and biota-environment linkage. *Journal of*
542 *Experimental Marine Biology and Ecology* 366:56–69. DOI: 10.1016/j.jembe.2008.07.009.
- 543 Cordes EE, Jones DOB, Schlacher TA, Amon DJ, Bernardino AF, Brooke S, Carney R, DeLeo

- 544 DM, Dunlop KM, Escobar-Briones EG, Gates AR, Génio L, Gobin J, Henry LA, Herrera S,
545 Hoyt S, Joye M, Kark S, Mestre NC, Metaxas A, Pfeifer S, Sink K, Sweetman AK, Witte U.
546 2016. Environmental impacts of the deep-water oil and gas industry: A review to guide
547 management strategies. *Frontiers in Environmental Science* 4. DOI:
548 10.3389/fenvs.2016.00058.
- 549 Davies AJ, Guinotte JM. 2011. Global habitat suitability for framework-forming cold-water
550 corals. *PloS one* 6:e18483.
- 551 Dickson AG, Sabine CL, Christian JR. 2007. *Guide to best practices for ocean CO2*
552 *measurements*. North Pacific Marine Science Organization.
553 <https://www.oceanbestpractices.net/handle/11329/249>
- 554 Everett M V., Park LK. 2018. Exploring deep-water coral communities using environmental
555 DNA. *Deep Sea Research Part II: Topical Studies in Oceanography* 150:229–241. DOI:
556 10.1016/J.DSR2.2017.09.008.
- 557 Georgian SE, DeLeo D, Durkin A, Gomez CE, Kurman M, Lunden JJ, Cordes EE. 2016a.
558 Oceanographic patterns and carbonate chemistry in the vicinity of cold-water coral reefs in
559 the Gulf of Mexico: Implications for resilience in a changing ocean. *Limnology and*
560 *Oceanography* 61:648–665.
- 561 Georgian SE, Dupont S, Kurman M, Butler A, Strömberg SM, Larsson AI, Cordes EE. 2016b.
562 Biogeographic variability in the physiological response of the cold-water coral *Lophelia*
563 *pertusa* to ocean acidification. *Marine Ecology* 37:1345–1359. DOI: 10.1111/maec.12373.
- 564 Georgian SE, Shedd W, Cordes EE. 2014. High-resolution ecological niche modelling of the
565 cold-water coral *Lophelia pertusa* in the Gulf of Mexico. *Marine Ecology Progress Series*
566 506:145–161. DOI: 10.3354/meps10816.

- 567 Gleckler PJ, Durack PJ, Stouffer RJ, Johnson GC, Forest CE. 2016. Industrial-era global ocean
568 heat uptake doubles in recent decades. *Nature Climate Change* 6:394–398. DOI:
569 10.1038/nclimate2915.
- 570 Gómez CE, Wickes L, Deegan D, Etnoyer PJ, Cordes EE. 2018. Growth and feeding of deep-sea
571 coral *Lophelia pertusa* from the California margin under simulated ocean acidification
572 conditions. *PeerJ* 2018. DOI: 10.7717/peerj.5671.
- 573 Guinotte JM, Orr J, Cairns S, Freiwald A, Morgan L, George R. 2006. Will human-induced
574 changes in seawater chemistry alter the distribution of deep-sea scleractinian corals?
575 *Frontiers in Ecology and the Environment* 4:141–146.
- 576 Henry LA. 2011. A deep-sea coral ‘gateway’ in the northwestern Caribbean. *Palomares MLD,*
577 *Pauly D Too Precious to Drill: the Marine Biodiversity of Belize*:120–124.
- 578 Hernández-Ávila I. 2014. Patterns of deep-water coral diversity in the Caribbean basin and
579 adjacent southern waters: An approach based on records from the R/V Pillsbury
580 expeditions. *PLoS ONE* 9. DOI: 10.1371/journal.pone.0092834.
- 581 Huang W, Wang Y, Cai W. 2012. Assessment of sample storage techniques for total alkalinity
582 and dissolved inorganic carbon in seawater. *Limnology and oceanography: Methods*
583 10:711–717.
- 584 Jiang L, Feely RA, Carter BR, Greeley DJ, Gledhill DK, Arzayus KM. 2015. Climatological
585 distribution of aragonite saturation state in the global oceans. *Global Biogeochemical*
586 *Cycles* 29:1656–1673. DOI: 10.1002/2015GB005198.
- 587 Littler MM, Littler DS, Blair SM, Norris JN. 1986. Deep-water plant communities from an
588 uncharted seamount off San Salvador Island, Bahamas: distribution, abundance, and primary
589 productivity. *Deep-sea Research* 33:881–892.

- 590 Liu M, Tanhua T. 2019. Distribution of Water Masses in the Atlantic Ocean based on
591 GLODAPv2. *Ocean Science Discussions*:1–32. DOI: 10.5194/os-2018-140.
- 592 Love MS, Lenarz B, Snook L. 2010. A survey of the reef fishes, purple hydrocoral (*Stylaster*
593 *californicus*), and marine debris of Farnsworth Bank, Santa Catalina Island. *Bulletin of*
594 *Marine Science* 86:35–52.
- 595 Lunden JJ, Georgian SE, Cordes EE. 2013. Aragonite saturation states at cold-water coral reefs
596 structured by *Lophelia pertusa* in the northern Gulf of Mexico. *Limnology and*
597 *Oceanography* 58:354–362. DOI: 10.4319/lo.2013.58.1.0354.
- 598 Lutz SJ, Ginsburg RN. 2007. State of deep coral ecosystems in the Caribbean region: Puerto
599 Rico and the US Virgin Islands. *The State of Deep Coral Ecosystems of the United States*.
600 *NOAA Technical Memorandum CRCP-3, Silver Spring, MD*:307–365.
- 601 Messing CG, Neumann AC, Lang JC. 1990. Biozonation of Deep-Water Lithoherms and
602 Associated Hardgrounds in the Northeastern Straits of Florida. *Palaios* 5:15–33.
- 603 Miller KJ, Gunasekera RM. 2017. A comparison of genetic connectivity in two deep sea corals
604 to examine whether seamounts are isolated islands or stepping stones for dispersal.
605 *Scientific Reports* 7:1–14. DOI: 10.1038/srep46103.
- 606 Miller KA, Thompson KF, Johnston P, Santillo D. 2018. An Overview of Seabed Mining
607 Including the Current State of Development, Environmental Impacts, and Knowledge Gaps.
608 *Frontiers in Marine Science* 4:418. DOI: 10.3389/fmars.2017.00418.
- 609 Miloslavich P, Díaz JM, Klein E, Alvarado JJ, Díaz C, Gobin J, Escobar-Briones E, Cruz-Motta
610 JJ, Weil E, Cortés J, Bastidas AC, Robertson R, Zapata F, Martín A, Castillo J, Kazandjian
611 A, Ortiz M. 2010. Marine biodiversity in the caribbean: Regional estimates and distribution
612 patterns. *PLoS ONE* 5. DOI: 10.1371/journal.pone.0011916.

- 613 Montes E, Muller-karger FE, Cianca A, Lomas MW, Lorenzoni L, Habtes S. 2016. Decadal
614 variability in the oxygen inventory of North Atlantic subtropical underwater captured by
615 sustained, long-term oceanographic time series observations. *Global Biogeochemical Cycles*
616 30:460–478. DOI: 10.1002/2015GB005183.Received.
- 617 Morrison JM, Nowlin WD. 1982. General distribution of water masses within the eastern
618 Caribbean Sea during the winter of 1972 and fall of 1973. *Journal of Geophysical*
619 *Research: Oceans* 87:4207–4229.
- 620 OBIS. 2019. Ocean Biogeographic Information System. *Intergovernmental Oceanographic*
621 *Commission of UNESCO*.
- 622 Pérez FF, Fontela M, Garcia-Ibañez MI, Mercier H, Velo A, Lherminier P, Zunino P, de la Paz
623 M, Alonso-Pérez F, Guallart EF, Padin XA. 2018. Meridional overturning circulation
624 conveys fast acidification to the deep Atlantic Ocean. *Nature*. DOI: 10.1038/nature25493.
- 625 Quattrini AM, Demopoulos AWJ, Singer R, Roa-Varon A, Chaytor JD. 2017. Demersal fish
626 assemblages on seamounts and other rugged features in the northeastern Caribbean. *Deep*
627 *Sea Research Part I: Oceanographic Research Papers*. DOI: 10.1016/j.dsr.2017.03.009.
- 628 Raddatz J, Titschack J, Frank N, Freiwald A, Conforti A, Osborne A, Skornitzke S, Stiller W,
629 Rüggeberg A, Voigt S, Albuquerque ALS, Vertino A, Schröder-Ritzrau A, Bahr A. 2020.
630 *Solenosmilia variabilis*-bearing cold-water coral mounds off Brazil. *Coral Reefs* 39:69–83.
631 DOI: 10.1007/s00338-019-01882-w.
- 632 Ragnarsson SÁ, Burgos JM, Kutti T, Beld I Van Den, Egilsdóttir H, Arnaud-haond S, Grehan A.
633 2017. The impact of Anthropogenic Activity on Cold-Water Corals. In: Rossi S ed. *Marine*
634 *Animal Forests*. Springer International Publishing, 1–35. DOI: 10.1007/978-3-319-17001-5.
- 635 Reed JK, Messing C, Walker BK, Brooke S, Correa TBS, Brouwer M, Udouj T, Farrington S.

- 636 2013. Habitat Characterization, Distribution, and Areal Extent of Deep-sea Coral
637 Ecosystems off Florida, Southeastern U.S.A. *Caribbean Journal of Science* 47:13–30. DOI:
638 10.18475/cjos.v47i1.a3.
- 639 Reed JK, Weaver DC, Pomponi SA. 2006. Habitat and fauna of deep-water *Lophelia pertusa*
640 coral reefs off the southeastern US: Blake Plateau, Straits of Florida, and Gulf of Mexico.
641 *Bulletin of Marine Science* 78:343–375.
- 642 Reyes J, Santodomingo N, Gracia A, Borrero-Pérez G, Navas G, Mejía-Ladino LM, Bermúdez
643 A, Benavides M. 2005. Southern Caribbean azooxanthellate coral communities off
644 Colombia. In: *Cold-water corals and Ecosystems*. Springer, 309–330.
- 645 Robbins LL, Hansen ME, Kleypas JA, Meylan SC. 2010. *CO2calc: A user-friendly seawater*
646 *carbon calculator for Windows, Mac OS X, and iOS (iPhone)*. US Geological Survey.
- 647 Roberts JM, Wheeler A, Freiwald A, Cairns SD. 2009. *Cold-water corals: the biology and*
648 *geology of deep-sea coral habitats*. Cambridge University Press.
- 649 Rogers AD. 1994. The biology of seamounts. In: *Advances in marine biology*. Elsevier, 305–
650 350.
- 651 Rogers AD. 2018. The Biology of Seamounts: 25 Years on. *Advances in Marine Biology*
652 79:137–224. DOI: 10.1016/BS.AMB.2018.06.001.
- 653 Santodomingo N, Reyes J, Gracia A, Martínez A, Ojeda G, García C. 2007. Azooxanthellate
654 *Madracis* coral communities off San Bernardo and Rosario Islands (Colombian Caribbean).
655 *Bulletin of Marine Science* 81:273–287.
- 656 Schlitzer R. 2019. Ocean data view. Available at: <https://odv.awi.de/>
- 657 Schroeder WW, Brooke SD, Olson JB, Phaneuf B, McDonough JJ, Etnoyer P. 2005. Occurrence
658 of deep-water *Lophelia pertusa* and *Madrepora oculata* in the Gulf of Mexico. In: *Cold-*

- 659 *water corals and ecosystems*. Springer, 297–307.
- 660 Thresher RE, Tilbrook B, Fallon S, Wilson NC, Adkins J. 2011. Effects of chronic low carbonate
661 saturation levels on the distribution, growth and skeletal chemistry of deep-sea corals and
662 other seamount megabenthos. *Marine Ecology Progress Series* 442:87–99. DOI:
663 10.3354/meps09400.
- 664 Trotter JA, Pattiaratchi C, Montagna P, Taviani M, Falter J, Thresher R, Hosie A, Haig D,
665 Foglini F, Hua Q. 2019. First ROV exploration of the Perth Canyon: Canyon setting, faunal
666 observations, and anthropogenic impacts. *Frontiers in Marine Science*.
- 667 Venn A, Tambutté E, Holcomb M, Allemand D, Tambutté S. 2011. Live tissue imaging shows
668 reef corals elevate pH under their calcifying tissue relative to seawater. *PLoS ONE* 6. DOI:
669 10.1371/journal.pone.0020013.
- 670 Wagner D, Sowers D, Williams SM, Auscavitch S, Blaney D, Cromwell M. 2019. *Océano*
671 *Profundo 2018: Exploring deep sea habitats off Puerto Rico and the US Virgin Islands*.
- 672 Watling L, Norse EA. 1998. Disturbance of the Seabed by Mobile Fishing Gear: A Comparison
673 to Forest Clearcutting. *Conservation Biology* 12:1180–1197.
- 674
- 675
- 676

Figure 1

Multibeam bathymetric map of the Aneгада Passage seamounts.

The locations of Dog, Conrad, and Noroît Seamount are indicated in bold. Dive locations are overlaid in yellow and labeled by dive number. The bathymetry color ramp in the lower right indicates depth values measured in meters. Transect segments lengths are not drawn to scale.

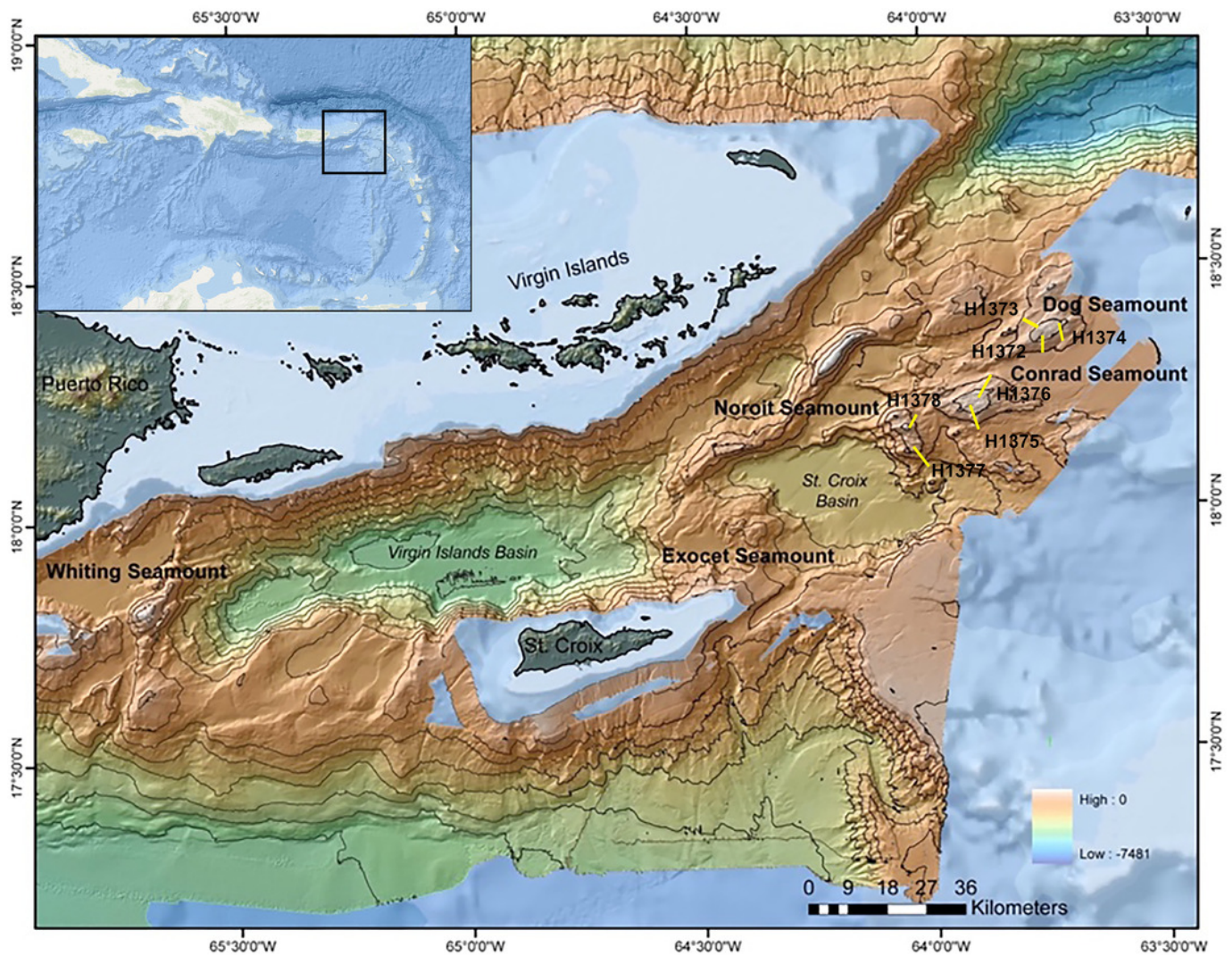


Figure 2

Temperature-Salinity plot for the Anegada Passage based on CTD water column profiles.

Water masses are overlaid and abbreviated by the following: SUW=Subtropical underwater, SSW=Sargasso Sea Water, TACW= Tropical Atlantic Central Water, AAIW=Antarctic Intermediate Water, and NADW=North Atlantic Deep Water. Isopycnal surfaces (σ_θ) are indicated in gray.

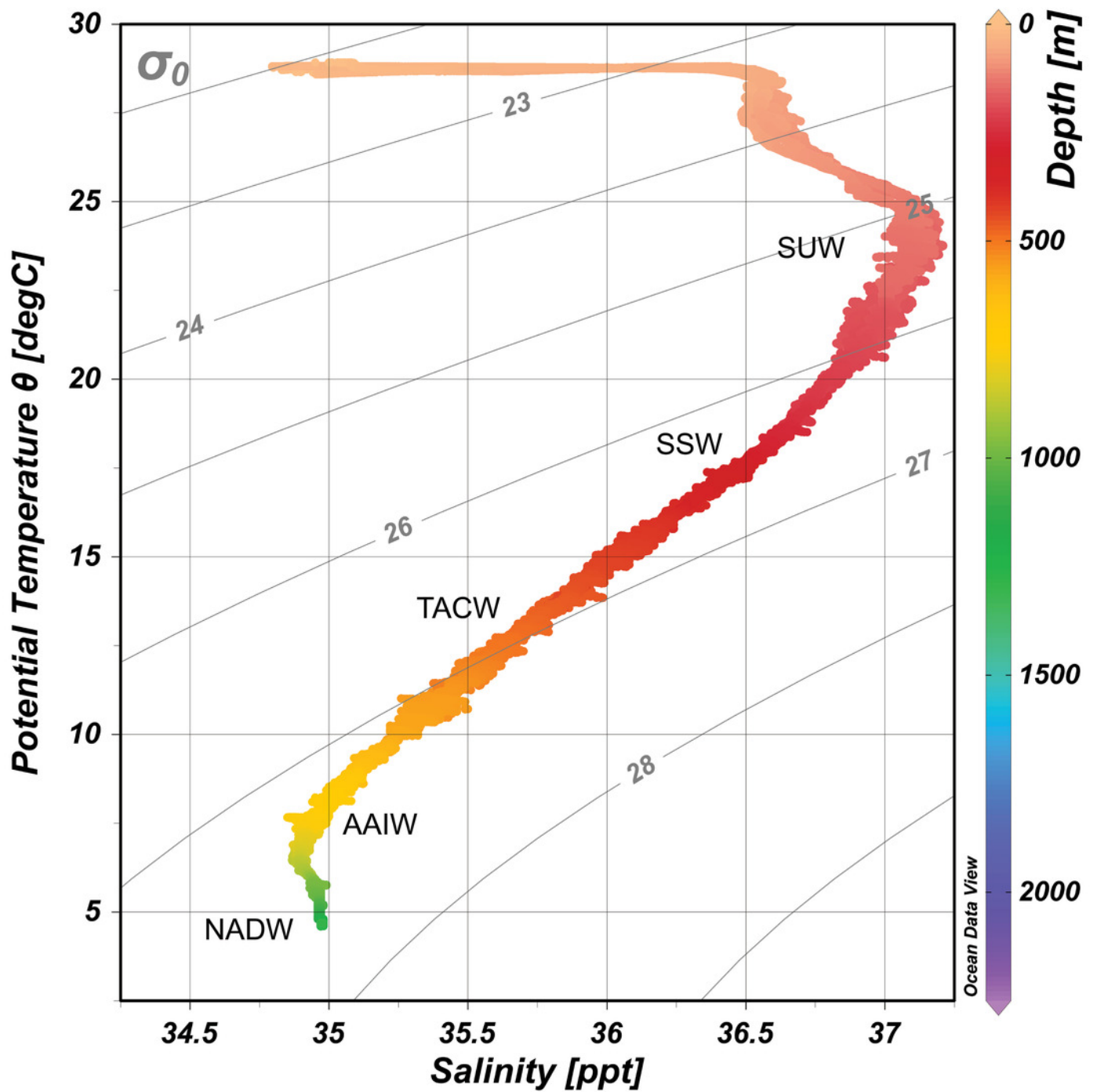


Figure 3

Depth distribution for scleractinian and stylasterid corals occurring on Dog, Conrad, and Noroît Seamounts.

Box plots represent the interquartile range with whiskers extending from the upper and lower quartiles to the minimum and maximum values. Horizontal lines represent the median depth. Individual points represent outliers. Species are arranged on the x-axis from shallowest to deepest by median depth of occurrence.

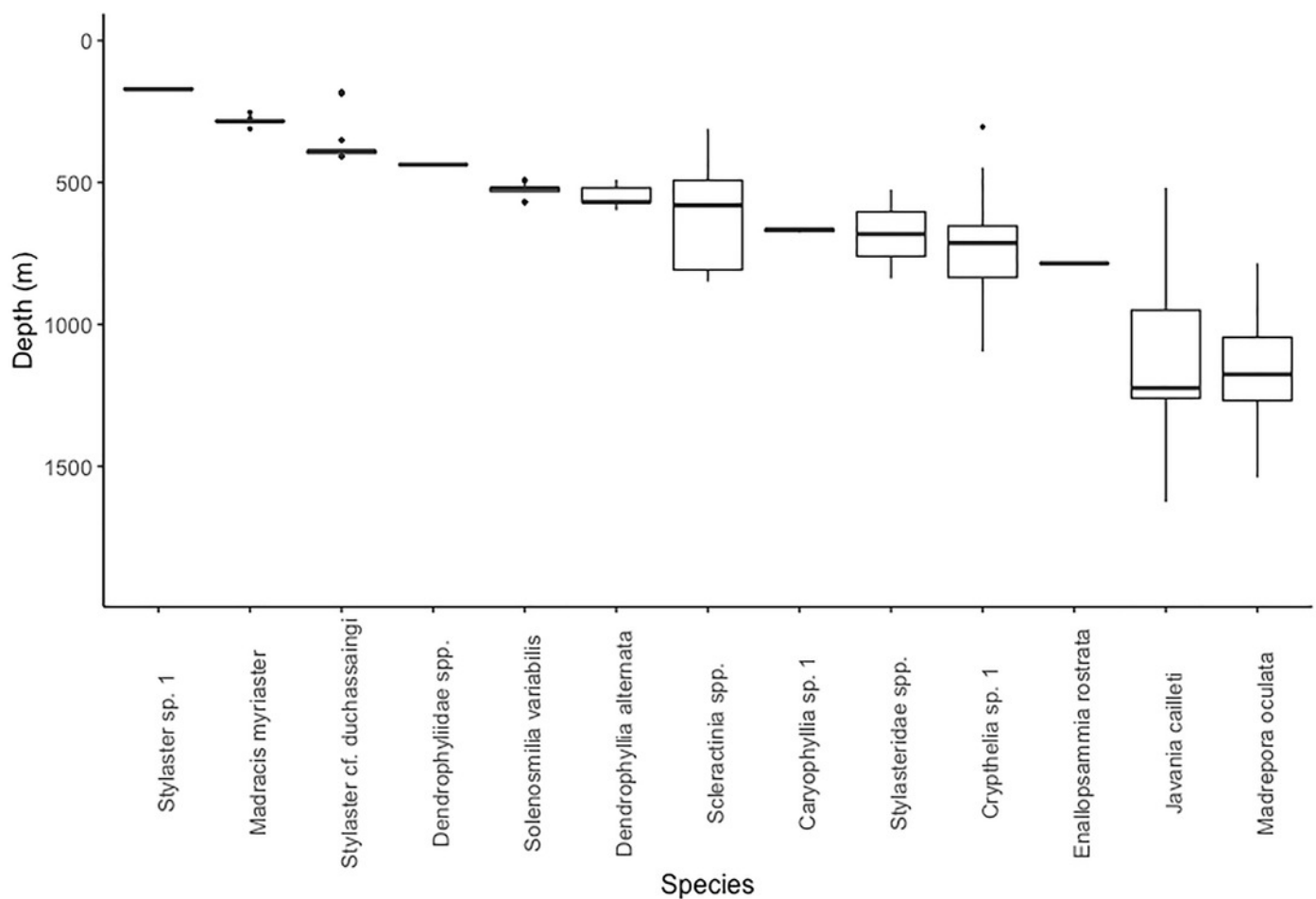


Figure 4

Distribution of scleractinian and stylasterid species against model predicted Ω_{Arag} values on the Anegada Passage seamounts.

Box plots represent the interquartile range with whiskers extending from the upper and lower quartiles to the minimum and maximum values. Vertical lines represent the median aragonite saturation state. Individual points represent outliers. Species are arranged on the y-axis from highest to lowest median aragonite saturation occurrence. A solid red vertical line indicates the aragonite saturation horizon, where $\Omega_{\text{Arag}} = 1$.

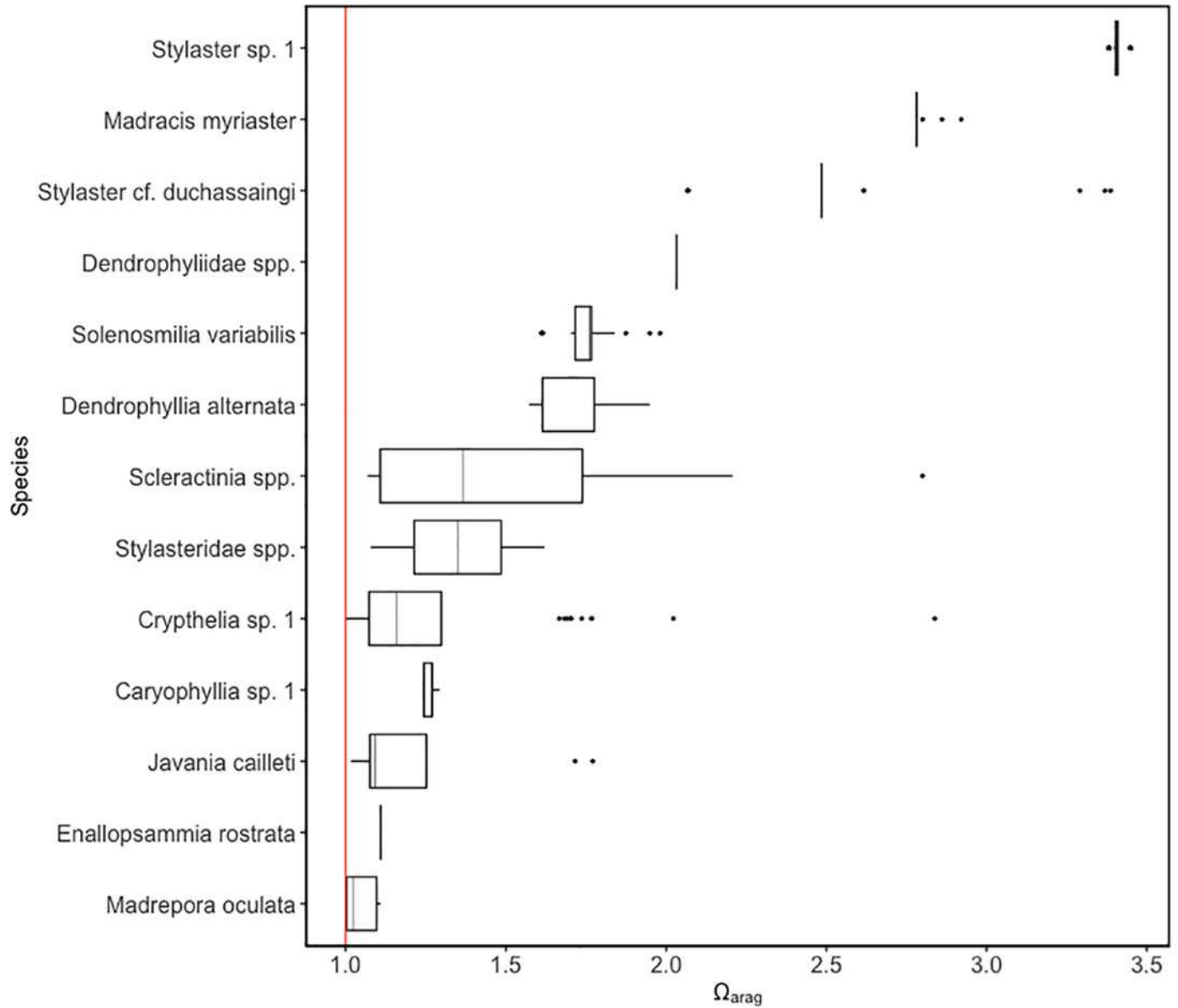


Figure 5

Species accumulation curves for the Anegada Passage seamounts.

Curves are plotted for all transects on Dog Seamount (276-1035 m), Conrad Seamount (162-1267 m), Noroit Seamount (881-2157 m), as well as for all three seamounts combined (162-2157 m).

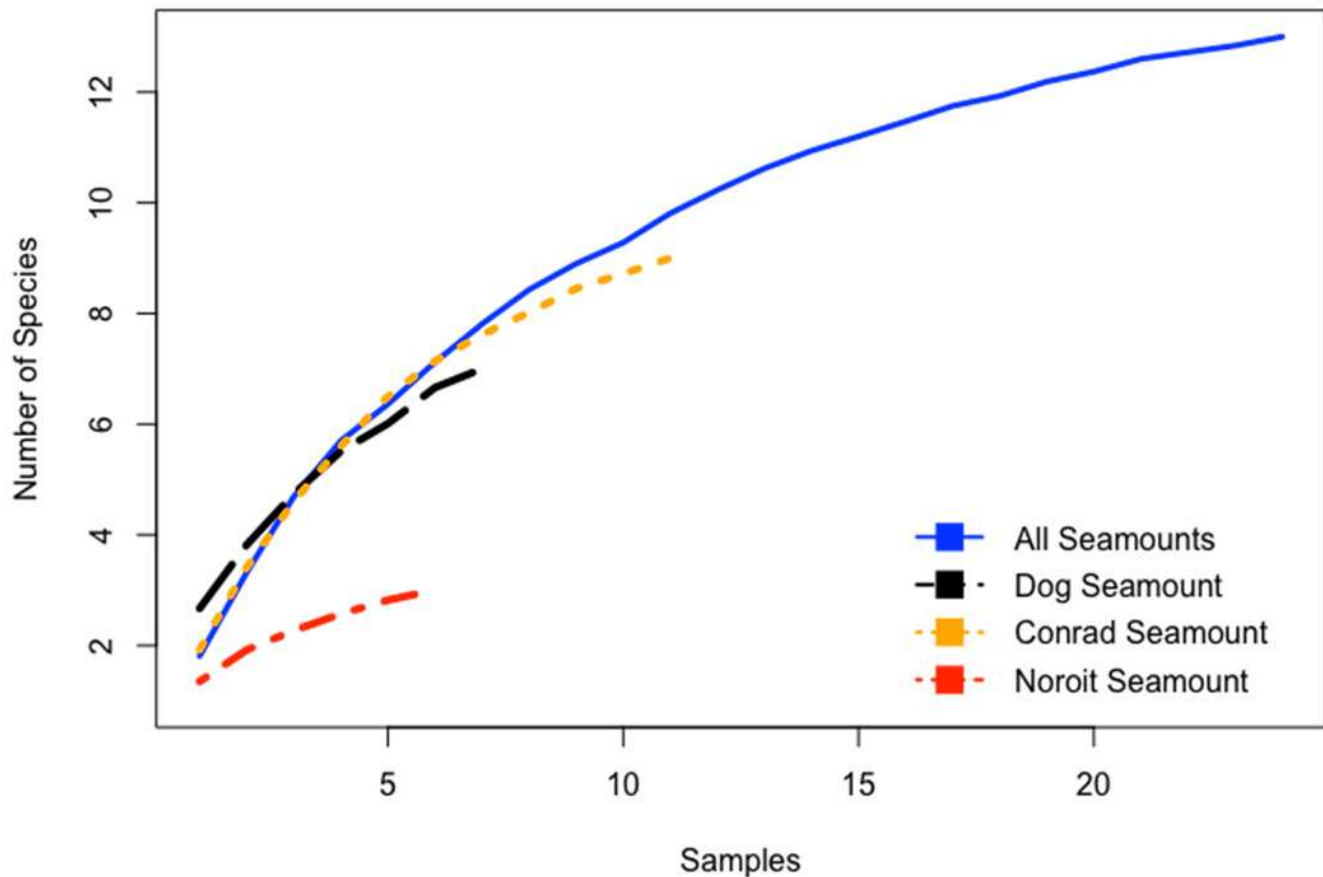


Figure 6

Non-metric multidimensional scaling analysis of standardized, fourth-root transformed coral assemblages on Dog, Conrad, and Noroît Seamounts.

SIMPROF groups are overlaid around significant groupings at the 95% level or above. Depth ranges displayed within each statistical grouping are indicated in black text.

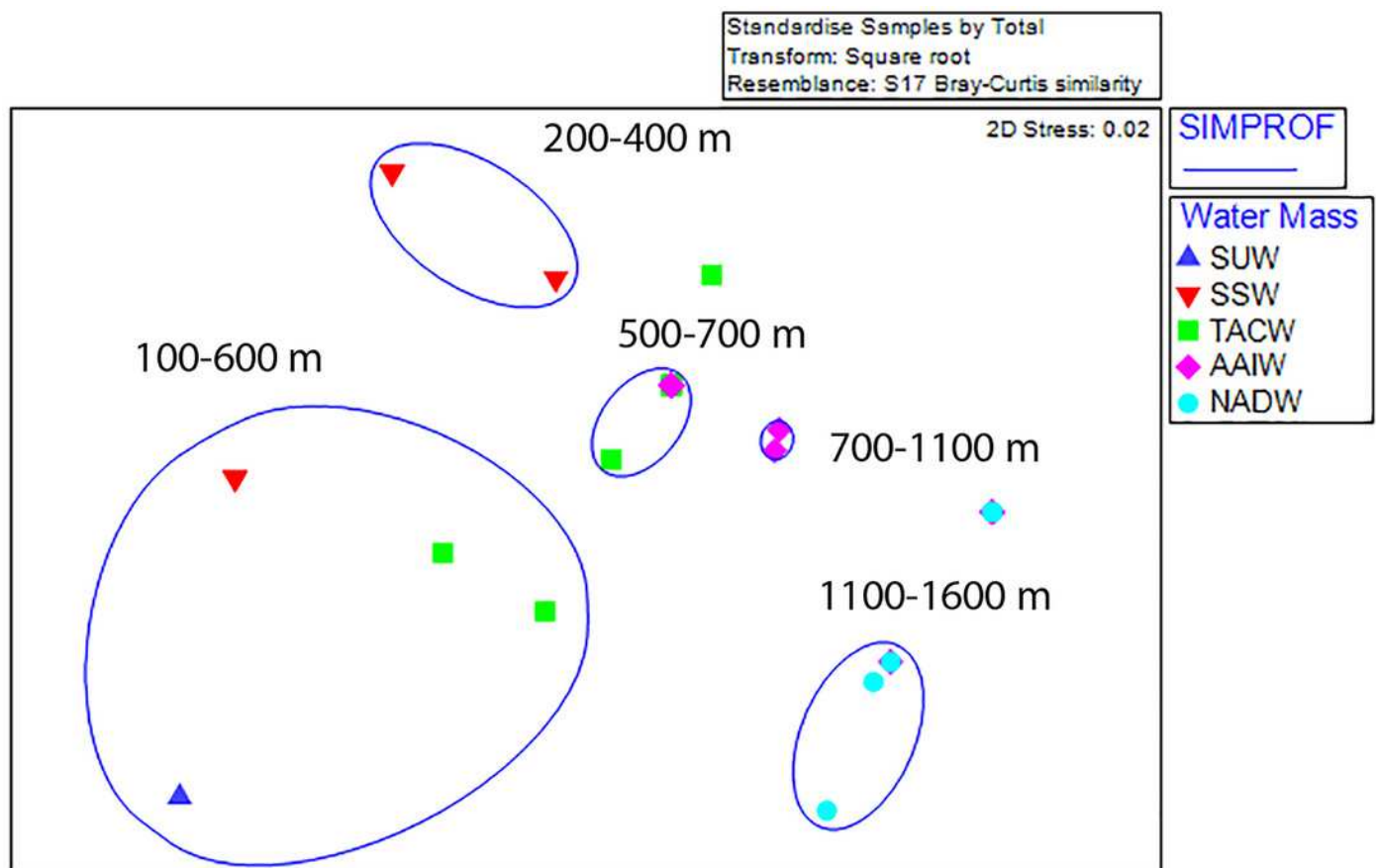


Figure 7

Distance-based linear model and redundancy analysis of coral assemblages and oceanographic variables.

Sample points represent one 100 m depth assemblage. Axes shown are the results of a distance-based redundancy analysis with percent variation explained by the first and second axes.

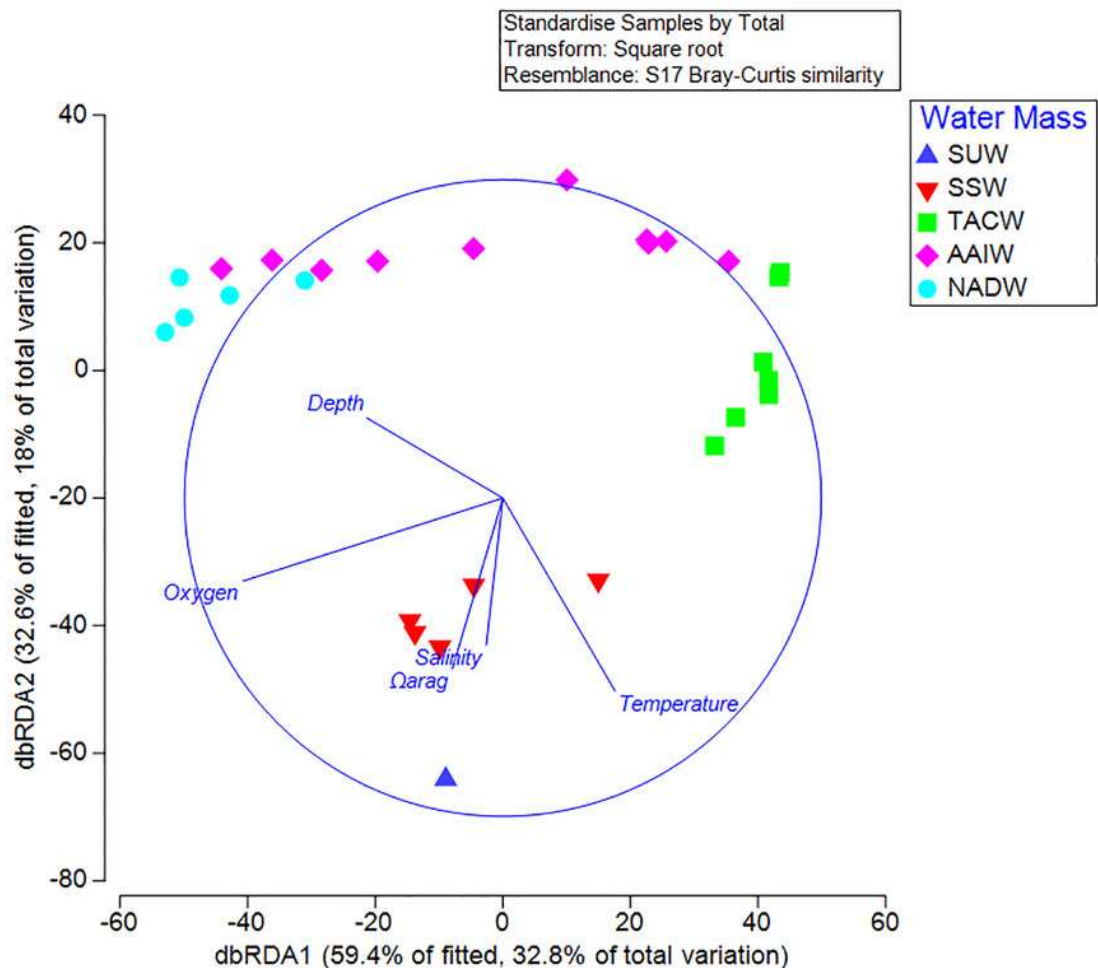


Figure 8

Deep-water scleractinians from the Aneгада Passage seamounts.

(A) *Enallopsammia rostrata*. (B) *Madrepora oculata*. (C) *Madracis myriaster*. (D) *Dendrophyllia alternata*. (E) *Javania cailleti*. (F) *Solenosmilia variabilis*.

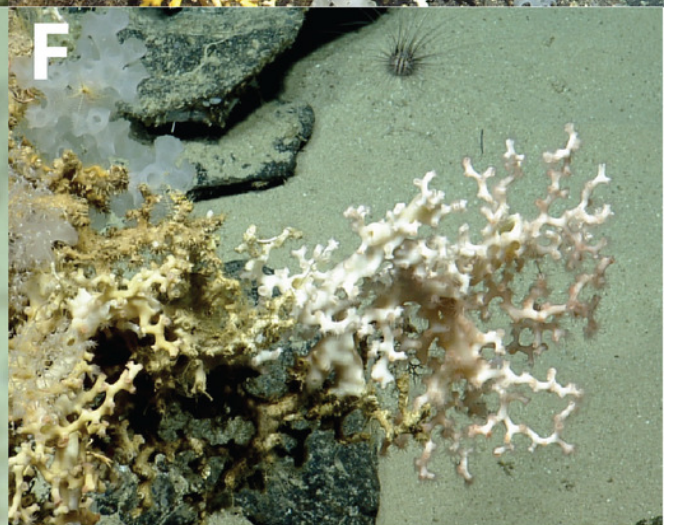
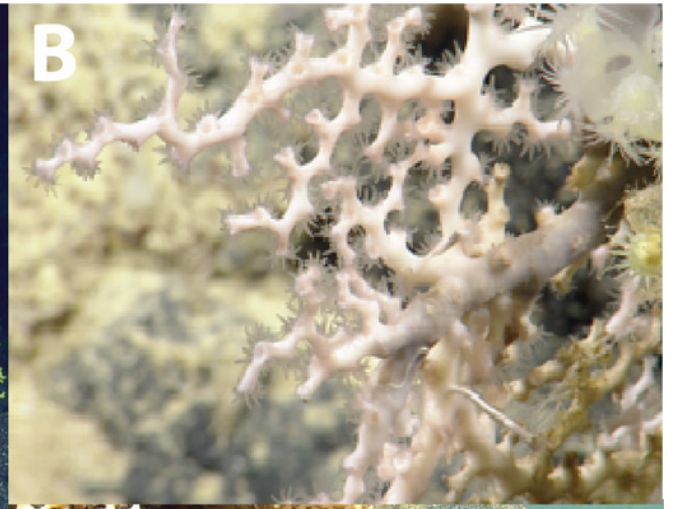
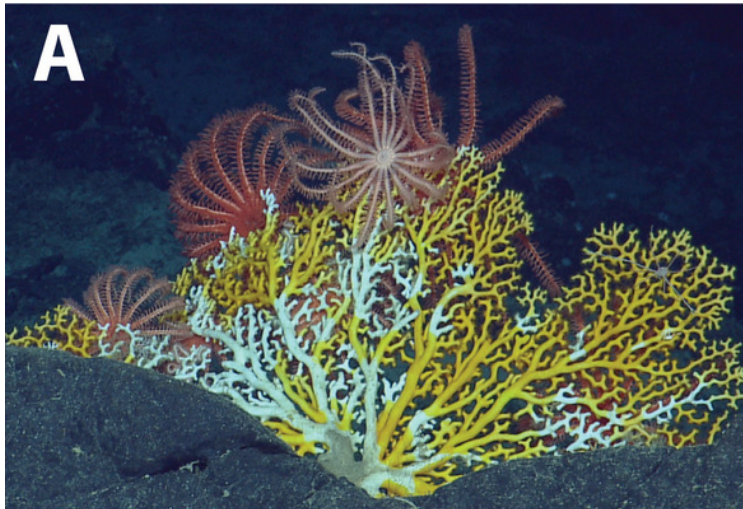


Figure 9

Deep-water stylasterids from the Aneгада Passage seamounts.

(A) *Crypthelia* sp. 1. (B) *Stylaster* cf. *duchassaingi*. (C) *Stylaster* sp. 1.

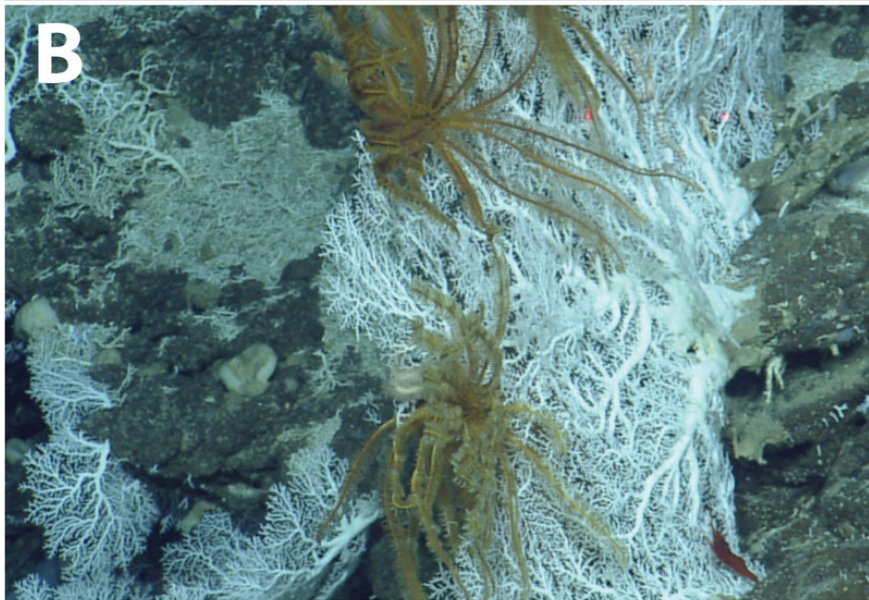
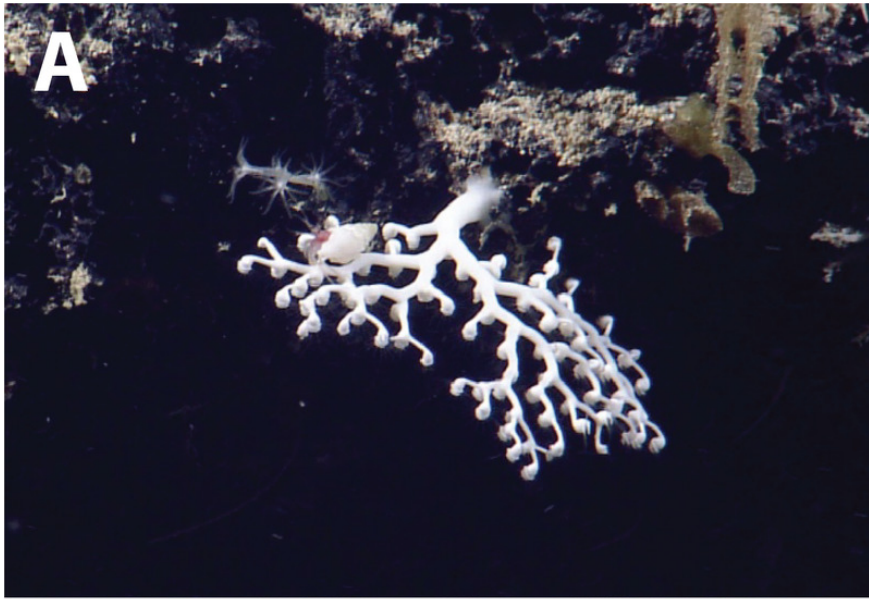


Table 1 (on next page)

ROV dive transect details for 2014 surveys of the Anegada Passage seamounts.

Start and end coordinates for each transect, time spent in visual contact with the seafloor, and number of water samples collected at depth over the dive interval are indicated.

- 1 Table 1: ROV dive transect details for 2014 surveys of the Anegada Passage seamounts. Start
- 2 and end coordinates for each transect, time spent in visual contact with the seafloor, and number
- 3 of water samples collected at depth over the dive interval are indicated.

Dive	Seamount	Start Coordinates	End Coordinates	Depth Range (m)	Number of Niskin Bottle Samples	Total Bottom Time (hh:mm)
H137 2	Dog	18°18.7385 N 63°46.0896 W	18°19.6177 N 63°46.1645 W	717-1035	6	07:56
H137 3	Dog	18°22.6480 N 63°46.1953 W	18°21.9711 N 63°45.9306 W	503-784	6	11:09
H137 4	Dog	18°20.4464 N 63°43.6091 W	18°21.9311 N 63°43.5024 W	276-601	5	09:58
H137 5	Conrad	18°10.5420 N 63°53.1020 W	18°13.0029 N 63°53.3459 W	162-876	5	31:40
H137 6	Conrad	18°16.4904 N 63°52.3364 W	18°14.2223 N 63°52.9767 W	344-1267	6	22:38
H137 7	Noroît	18° 05.4657 N 64° 00.1741 W	18° 07.0695 N 64° 01.1760 W	881-2157	6	17:10
H137 8	Noroît	18° 09.6969 N 64° 01.3606 W	18° 09.4122 N 64° 01.8888 W	949-1035	2	06:01

4

5

Table 2 (on next page)

Summary of records and environmental variables for each taxon.

Ranges of values for number of observations, depth, temperature, salinity, dissolved oxygen, model predicted Ω_{Arag} , and colony height are reported for each species by taxonomic grouping.

- 1 Table 2: Summary of records and environmental variables for each taxon. Ranges of values for number of observations, depth,
 2 temperature, salinity, dissolved oxygen, model predicted Ω_{Arag} , and colony height are reported for each species by taxonomic
 3 grouping.

Class	Family	Species	Number of observations	Depth (m)	Temperature (°C)	Salinity (psu)	Dissolved oxygen (mg/L)	Model Predicted Ω_{Arag}	Height (cm)
Hydrozoa	Stylasteridae	<i>Stylaster</i> sp. 1	65	166-174	22.1-22.5	37.00-37.05	7-7.12	3.38-3.45	-
		<i>Crypthelia</i> sp. 1	49	304-1096	4.9-18.0	34.53-36.55	2.41-7.22	0.99-2.83	1-12
		<i>Stylaster</i> cf. <i>duchassaingi</i>	30	181-408	13.8-22.1	35.82-37.01	5.39-6.99	2.07-3.39	12-37
		Stylasteridae spp.	2	525-838	6.7-10.9	34.89-35.39	4.96-5.28	1.08-1.62	3-5
Anthozoa	Caryophylliidae	<i>Solenosmilia variabilis</i>	44	490-569	10.9-13.3	35.37-35.75	4.88-5.15	1.61-1.98	12-18
		<i>Caryophyllia</i> sp. 1	3	665-677	8.2-8.7	35.03-35.07	4.78-4.86	1.24-1.29	-
	Oculinidae	<i>Madrepora oculata</i>	22	784-1540	4.3-6.9	34.53-34.97	5.22-8.23	1.00-1.10	10-125
	Pocilloporidae	<i>Madracis myriaster</i>	22	253-311	17.6-18.7	36.49-36.65	6.83-7.01	2.78-2.92	6-35
	<i>Incertae familiae</i>	Scleractinia spp. (solitary)	11	311-849	6.5-17.8	34.83-36.51	4.76-6.98	1.07-2.8	4-5
	Dendrophylliidae	<i>Dendrophyllia alternata</i>	5	490-598	10.7-13	35.33-35.71	4.84-5.13	1.57-1.95	16
		<i>Enallopsammia rostrata</i>	2	785	7.0	34.921	5.2	1.11	20-75
		Dendrophylliidae spp.	1	437	13.6	35.794	5.29	2.03	5
	Flabellidae	<i>Javania cailleti</i>	8	518-1626	4.2-12.0	34.557-35.54	4.96-8.34	1.02-1.77	4-7

4

5

Table 3 (on next page)

Summary of measured values of Ω_{Arag} from water samples taken directly adjacent to corals.

Sampling events are reported for each species arranged by taxonomic grouping.

- 1 Table 3: Summary of measured values of Ω_{Arag} from water samples taken directly adjacent to
 2 corals. Sampling events are reported for each species arranged by taxonomic grouping.

Class	Family	Species	Number of adjacent water samples	Ω_{Arag} measured
Hydrozoa	Stylasteridae	<i>Stylaster</i> sp. 1	0	-
		<i>Crypthelia</i> sp. 1	0	-
		<i>Stylaster</i> cf. <i>duchassaingi</i>	0	-
		Stylasteridae spp.	0	-
Anthozoa	Caryophylliidae	<i>Solenosmilia variabilis</i>	1	1.63
		<i>Caryophyllia</i> sp. 1	1	1.24
	Oculinidae	<i>Madrepora oculata</i>	2	1.13-1.16
	Pocilloporidae	<i>Madracis myriaster</i>	1	2.7
	<i>Incertae familiae</i>	Scleractinia spp. (solitary)	0	-
	Dendrophylliidae	<i>Dendrophyllia alternata</i>	1	1.35
		<i>Enallopsammia rostrata</i>	1	1.21
		Dendrophylliidae spp.	1	1.82
	Flabellidae	<i>Javania cailleti</i>	1	1.16

3